JOURNAL OF SOLID STATE CHEMISTRY 44, 374–381 (1982)

High-Resolution Electron Microscope Analysis of {100} Twinning in β-Rhombohedral Boron

M. J. McKELVY, A. R. RAE SMITH, AND L. EYRING*

Department of Chemistry and the Center for Solid State Science, Arizona State University, Tempe, Arizona 85287

Received March 30, 1982

{100} twinning in β-rhombohedral boron formed during rapid cooling of a multiphase mixture was reexamined by high-resolution electron microscopy. Comparison of observed and calculated images shows that the twin boundaries (which pass through the center of the B_{84} units in the structure) occur in pairs, separated by one to five unit cells of the twinned orientation. Twinned regions are typically separated by 100 to 500 Å. The twin boundary pairs may also be described as stacking faults in the pseudocubic close-packed arrangement formed by the B_{84} units, which are pseudospherical in symmetry.

Introduction

The crystal structure of β-rhombohedral boron was first determined by Hughes *et al.* (*1*), with further analysis and refinement by two independent sets of workers (*2*). It is based on an interconnecting network of B_{12} icosahedra. These icosahedral units are a fundamental building block of boron and boride chemistry. A later and more accurate determination was made by Callmer (*3*) for a structural comparison of solid solutions of metals in β-rhombohedral boron to β-rhombohedral boron itself.

Several low-resolution transmission electron microscopy studies have revealed the existence of interesting structural defects. Kleinhenz and Runow observed {100} twinning and {10$\bar{1}$} stacking faults in samples thinned by chemical etching and cathode sputtering (*4*). Similar observations were made by other workers (*5*). Twinning was also observed by Tavadze *et al.* in a study of the structural perfection of β-rhombohedral boron prepared by zone melting (*6*). Extensive {100} twinning has also been observed in the α-rhombohedral modification of boron (*7*).

In this paper, we present high-resolution electron microscopy (HRTEM) results which further elucidate {100} twinning in β-rhombohedral boron. These observations were made in the course of an investigation of the nonstoichiometric lanthanum borides $LaB_{6+\delta}$, containing elemental boron.

Experimental

The sample used in this investigation was provided by Dr. Edmund Storms[1] and contained comparable amounts of $LaB_{6+\delta}$ and elemental boron. Details of its preparation by arc melting of elemental lanthanum and boron have been described (*8*). It is likely

* Author to whom correspondence should be addressed.

[1] Los Alamos Scientific Laboratory of the University of California, Los Alamos, New Mexico.

0022-4596/82/120374-08$02.00/0

that this arc-melted boron contains a greater concentration of the defect being studied than would the zone-melted samples used in some of the earlier structural or defect studies. The chief impurity was 0.1–0.2 weight% carbon, with several hundred ppm of oxygen, 500 ppm silicon, and 200 ppm iron also present. Electron microprobe examination of the sample showed that the iron was present at grain boundaries or in association with the elemental boron, as it is before reaction. Further analysis led to the conclusion that the iron content had not increased significantly in the elemental boron during the boride preparation. Efforts to determine if the silicon had undergone any impurity segregation during sample preparation were inconclusive. However, even if all the silicon remained in the elemental boron, the concentration would be only one silicon atom in every ten unit cells of boron.

The specimens for HRTEM study were prepared by grinding the sample in an agate mortar under liquid nitrogen to aid formation of thin crystal edges suitable for HRTEM observation (*9*). The crystals were then suspended in acetone and dried onto thin holey carbon film grids. A thin surface layer of gold had been previously evaporated on the grids giving independent polycrystalline islands of gold approximately 200 Å in diameter. These islands acted as an internal electron diffraction standard. The β-rhombohedral boron crystals observed in this study were characterized from their ⟨100⟩ diffraction patterns using the known lattice parameters and the internal gold standard. Agreement between observed and calculated *d*-spacings was within experimental error (<1%). The HRTEM observations were made on a JEOL JEM 100B electron microscope capable of a point-to-point resolution of 3.4 Å.

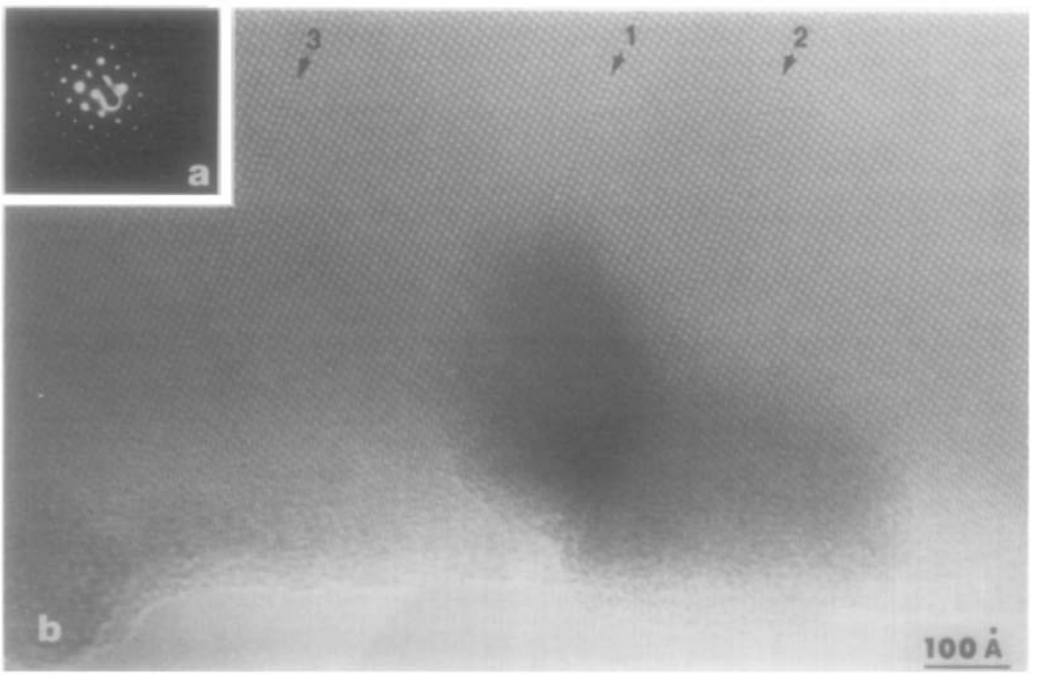

FIG. 1. (a) A [001] diffraction pattern of faulted β-rhombohedral boron, showing streaking in the [100] direction. (b) A low-magnification [001] image of (100) planar faults in β-rhombohedral boron (indicated by arrows).

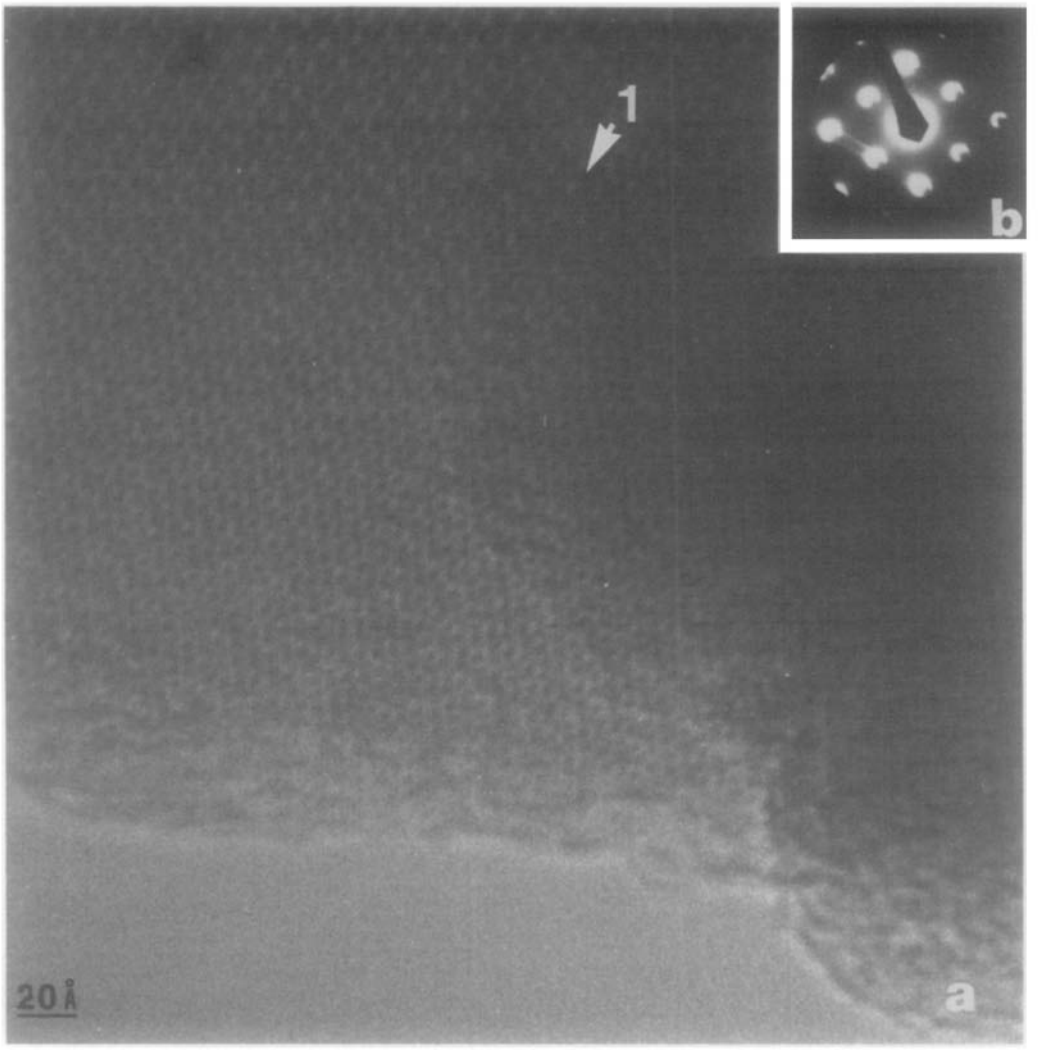

FIG. 2. (a) An enlargement of fault 1 in Fig. 1b near the edge of the crystal. (b) A diffraction pattern obtained in imaging the area in (a), showing the displacement of the objective aperture.

Calculations of projected atomic positions, electron diffraction patterns, and HR-TEM images were carried out on a Data General Eclipse S/140 minicomputer using an interactive system described elsewhere (*10*). The atomic coordinates and occupancy factors used were those determined by Callmer (*3*).

Image Comparison and Analysis

The elemental boron crystals observed in the electron microscope were almost exclusively of the high-temperature β-rhombohedral modification. The lattice dimensions corresponded to those quoted in the literature (*3*) to within 1%. Because of multiple diffraction, the diffracted beam intensities were not those expected from kinematic considerations (in particular, very weak {100} and {110} intensities were predicted). However, the image agreement described below confirms the nature of these crystals.

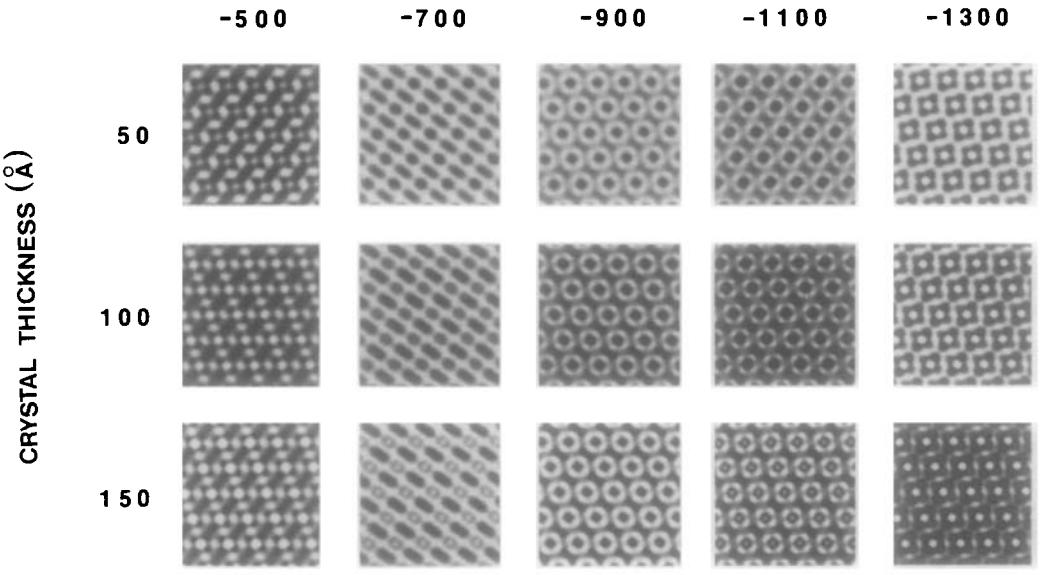

FIG. 3. A through focus/thickness series of calculated ⟨100⟩ images for the unfaulted structure.

For some of the boron crystals, a streaking in the [100] direction of the [001] diffraction pattern was observed (Fig. 1a). This type of streaking is characteristic of stacking faults perpendicular to the streaked direction, and examination of the images at relatively low magnification does indeed show (100) planar faults (Fig. 1b).

Closer examination of the faulted areas at higher magnification (Fig. 2a) shows that they consist of a thin region between one and five unit cells thick with parallel boundaries which extend into the body of the crystal. The structure on either side of the faulted region has the same orientation, with a relative displacement along the [010] direction. The faulted region is related to the main structure by reflection across the shared (100) planes. Measurement of the projected cell dimensions and angle (73°) indicated that the internal structure is identical to the main structure within experimental error. Thus the fault planes are actually (100) twin boundaries. Because the faulted regions are rarely more than two unit cells in thickness, the alternative orientation does not appear in the diffraction pattern as distinct spots.

To confirm this, the observed micrographs were compared with calculated images based on this model. Initially the unfaulted region near the crystal edge was

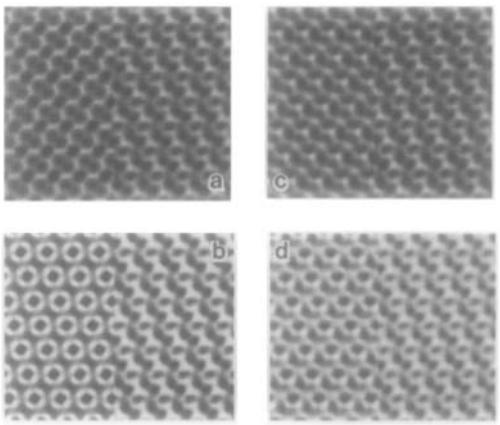

FIG. 4. A comparison of the unfaulted structure (enhanced by averaging) with calculated images (which form the left half of each pair). (a) Aperture radius 0.225 $Å^{-1}$. (b) Aperture radius 0.23 $Å^{-1}$. (c and d) Aperture radius 0.225 $Å^{-1}$, displacement 0.017 $Å^{-1}$ along [100]. (c) Defocus −650 Å. (d) Defocus −1050 Å.

used for comparison. Calculations were carried out from 0 to 1300 Å under focus and for crystal thicknesses of 50, 100, and 150 Å. A selection is shown in Fig. 3. The parameters used in the calculation were: spherical aberration constant, 1.8 mm; depth of focus, 200 Å; beam divergence angle, 2 mrad; aperture radius, 0.23 $Å^{-1}$. The features of the calculated image do not change much with thickness or with defocus between 750 and 1050 Å under focus, but the experimental images show some asymmetry not present in the calculated images. This is because the objective aperture used in the imaging cut through eight intense diffracted beams (d-spacings 0.222 $Å^{-1}$ {210} and 0.228 $Å^{-1}$ {200}). The diffraction pattern used for obtaining the image in Fig. 2a is shown in Fig. 2b, and it can be seen that the beams do not contribute equally. When this is accounted for by displacing the center of the aperture in the calculations, the agreement is much more satisfactory. Figure 4 shows the comparison between the observed micrograph and the calculated images. In this figure, a small area of the experimental micrograph (about 30 unit cells) has been digitally averaged to enhance the image quality (the procedure has been described elsewhere (*10*)). Two defocus conditions give acceptable matches for the displaced aperture calculation. The fractional mean absolute difference (calculated on a point-to-point comparison) is 0.10 for 650 Å and 0.11 for 1050 Å under focus, compared with 0.13 for the two calculations with a centered aperture also shown (aperture radius 0.225 and 0.23 $Å^{-1}$).

Modeling and Image Calculation of the Twin Boundary

The image calculation programs (based on the Cowley–Moodie multislice method (*11*)) assume a periodic lattice characterized by the crystallographic unit cell. However, defects which are parallel to the beam direction have a relatively short-range effect on the appearance of the image. It is thus possible to construct a large artificial unit cell from the parent structure which contains the defect, and so obtain valid images to compare with the micrograph (*12*). The interactive program system (*10*) used in this analysis allows the building of such a model cell with relative ease. It was decided to model a cell which contained one unit cell of twinned orientation surrounded on either side by two cells of the normal orientation. This leaves five unit cells between each fault, quite sufficient for this purpose. The relationship of the defect cell to the parent structure is shown in Fig. 5. A brief description of the process of the modeling follows.

The calculation of the 555 atomic positions in this model cell would be tedious to carry out manually. The program makes the generation much easier. The cell can be assembled in a few simple stages. First, the atomic positions and symmetry operators for a single unit cell of β-rhombohedral boron were typed in using the values given by Callmer (*3*). Then, two cells with the dimensions of the final defect cell were generated which contained the two orientations of boron by giving the program the transformation matrices for the cell axes. These are given by the following equations: $X' = 5X - 0.59Y - 0.59Z$, $Y' = Y$, $Z' = Z$ for the main orientation, and $X' = 5X - 2.36Y - 2.36Z$, $Y' = -Y$, $Z' = -Z$ for the twin ori-

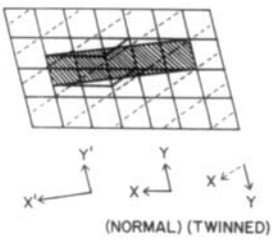

FIG. 5. A diagram showing the relationship between the cell used to model the defect and the two orientations of β-rhombohedral boron.

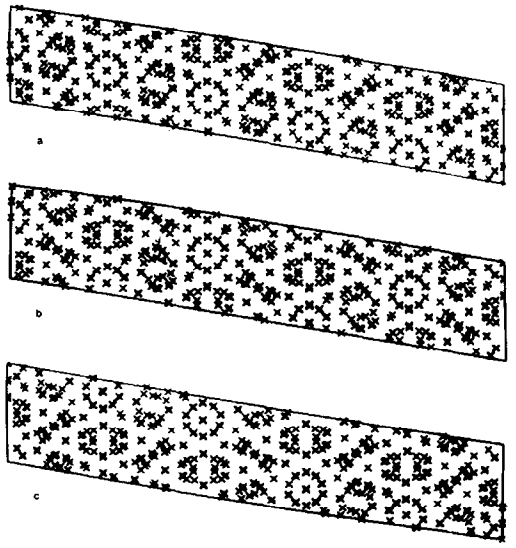

FIG. 6. The projected atom positions down the [001] direction. (a) A model cell containing normal orientation cells of boron. (b) A model cell containing twinned orientation cells of boron. (c) The final cell containing the twin boundary used for calculation (produced from combination of (a) and (b)).

entation. The atoms in each orientation which do not form part of the final cell were then rejected. For the main orientation, the atoms on the far side of the twin boundary ($X = 0.6 - 1.0$) were given an additional translational shift of (0, −0.59, −0.59) to ensure the correct matching at the boundaries with the twin orientation and the unit cell edge. The two sets of atoms thus generated were combined with the set of atoms in the twin orientation, which were given a translational shift of (0, 1.18, 1.18) for match at the boundaries. Plots of the atomic positions projected down the beam direction for the two orientations and the final defect cell are shown in Fig. 6 for clarity. Calculations were then carried out as for the unfaulted region. The comparison is shown in Fig. 7. The micrograph has been enhanced in this case by averaging along one lattice dimension only. There is more asymmetry in the experimentally averaged region (due to the slight displacement of the objective aperture), but the agreement is quite satisfactory, thus confirming the nature of the defect. In the original micrograph (shown in Fig. 1b), there are three such faults, indicated by arrows. Faults 1 and 2 are identical in origin, having a single unit cell width of the twin orientation. Fault 3 has two unit cells width in the twinned region. A model for fault 3 was calculated on the same lines as the single unit cell width defect, and the agreement was good as expected.

Discussion of the Crystal Structure

The structure of β-rhombohedral boron has been determined by single-crystal X-ray crystallography (*3*). It consists of two main building blocks, B_{84} and B_{21} units. Each B_{84} unit contains a regular icosahedron of 12 boron atoms at its center with each atom bonded to the apical boron atom of a pentagonal pyramid of boron atoms (which form a B_6 unit). These 84 atom units are pseudospherical in symmetry, and are centered on the corners of the rhombohedral unit cell ($a = 10.14$ Å, $\alpha = 65.2°$). They bond to each other along the ⟨100⟩ directions by two B_6 units forming an interlocking icosahedron. This net of B_{84} "spheres" forms a pseudocubic close-packed arrangement.

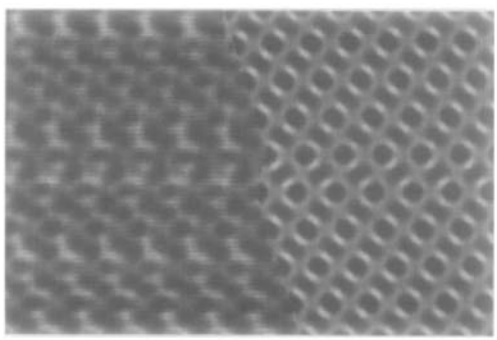

FIG. 7. A comparison of defect 1 (Fig. 1b) enhanced by one-dimensional averaging with the calculated image.

The B_{21} units fill the resultant octahedral space in the center of the unit cell. Each B_{21} unit has a central boron atom octahedrally coordinated to two B_{10} units, which are themselves formed from three condensed B_6 units. These condensed B_6 units bond icosahedrally to those B_6 units on the B_{84} "spheres" which are not directed along the ⟨100⟩ directions.

The X-ray study also indicates that the six boron positions surrounding the boron atom at the center of the cell have an average occupancy of 0.73, and suggests a partially occupied interstitial boron site in the B_{84} units. These latter features are too subtle to affect the HRTEM images and so will not be considered further.

The major structural features show up clearly in the HRTEM images. The dark spots at the center of the light rings correspond to the central icosahedra of the B_{84} units, which are located at the corners of the unit cell. The light rings surrounding these spots correspond to the relatively lower atom density around the icosahedra, as can be seen in the plot of the ⟨100⟩ projected atom positions (Fig. 8). The dark regions along the long unit cell diagonal correspond to the B_{21} units.

At the (100) twin boundary, which passes through the center of the B_{84} "spheres," the bonding of the B_6 units directed along the [100] direction changes. Instead of bonding to the next B_{84} unit, the [100] B_6 unit bonds icosahedrally to a B_{21} unit, while the B_6 unit which previously bonded to a B_{21} unit (the (100) mirror image of the [$\bar{1}$00] B_6 unit) now bonds icosahedrally to the next B_{84} unit. The B_{21} units on either side of the twin boundary have a mirror relationship across (100). In the [010] and [001] directions the B_{84} "spheres" continue to bond icosahedrally as in the parent structure.

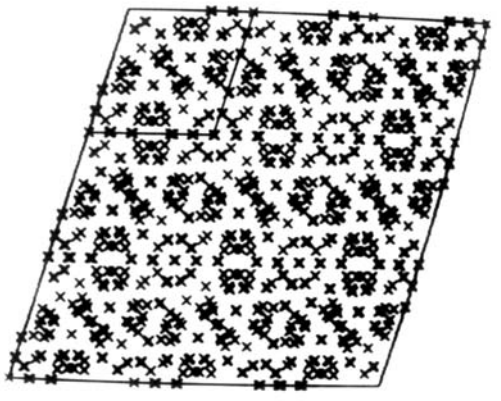

FIG. 8. The atom positions for β-rhombohedral boron projected down the ⟨100⟩ direction. The unit cell (a = 10.14 Å) is outlined.

The high symmetry of the B_{84} units and the similarity of the two types of bonding of their B_6 units (which form interlocking icosahedra with other B_6 units, whether belonging to another B_{84} unit or to a B_{21} unit) no doubt facilitate the twinning.

By considering the structure as a cubic close-packed array of B_{84} "spheres" with B_{21} units filling the octahedral interstices, the twin boundary pairs may be viewed in another light. The {100} planes of the rhombohedral cell are also the close-packed planes in the cubic close-packed array (the rhombohedral angle in the equivalent pseudo-face-centered cubic cell is 94.3°). If the normal stacking sequence of close-packed planes is represented as ABCABC . . . , then faults 1 and 2 correspond to a stacking sequence AB<u>CB</u>CABC . . . and fault 3 as AB<u>CBA</u>BC . . . (the twinned regions are underlined). This is illustrated for fault 1 in Fig. 9. This type of stacking fault is very common in many materials with close-packed structures.

Conclusions

The agreement between the calculated and observed images of the defects in crystalline β-rhombohedral boron confirm their nature as {100} twin boundaries as proposed by earlier workers. In these high-resolution studies, the twin boundaries occur

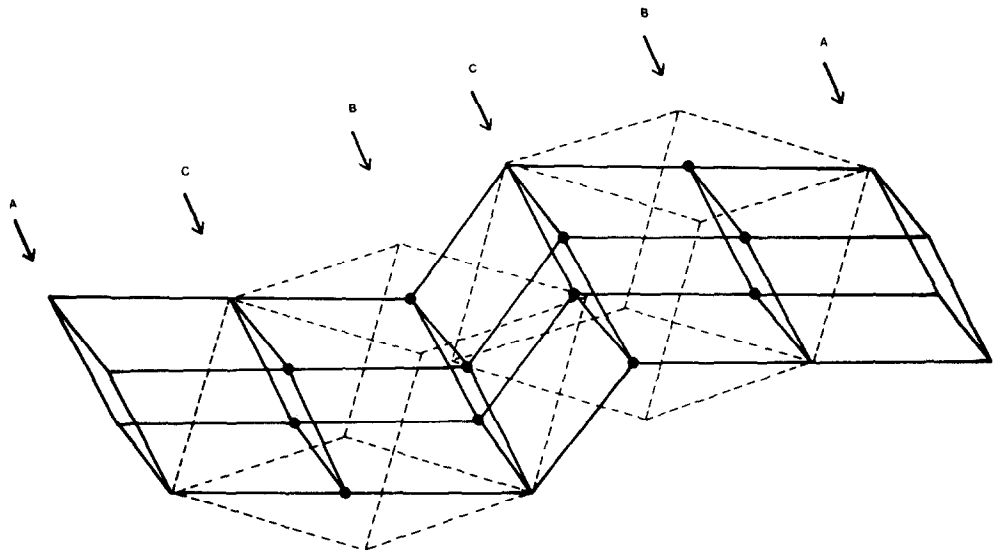

FIG. 9. An illustration of faults 1 and 2 showing the relationship of close-packed planes of the rhombohedral unit cell and the face-centered cubic cell.

in pairs, passing through the center of the B_{84} "spheres," and are separated by one to five unit cells of the twinned orientation (10 to 50 Å). The chemical impurities are not expected to be concentrated along the boundaries since, were this the case, the large atomic number difference between boron and its impurities would have had an effect on the appearance of the image.

Acknowledgment

It is a pleasure to acknowledge the support of the National Science Foundation through Grant DMR 81-08306 for the experimental work. The National Science Foundation through Grant CHE-7916098 supports the microscope facility used (The Regional Instrumentation Center for High Resolution Electron Microscopy).

References

1. R. E. HUGHES, C. H. L. KENNARD, D. B. SULLENGER, H. A. WEAKLIEM, D. E. SANDS, AND J. L. HOARD, *J. Amer. Chem. Soc.* **85**, 361 (1963).
2. J. L. HOARD, D. B. SULLENGER, C. H. L. KENNARD, AND R. E. HUGHES, *J. Solid State Chem.* **1**, 268 (1970); V. D. GEIST, R. KLOSS, AND H. FOLLNER, *Acta Crystallogr. Sect. B* **26**, 1800 (1970).
3. B. CALLMER, *Acta Crystallogr. Sect. B* **33**, 1951 (1977).
4. K. KLEINHENZ AND P. RUNOW, *Phys. Status Solidi* **29**, 627 (1968).
5. H. BINNENBRUCK, A. HAUSEN, P. RUNOW, AND H. WERHEIT, *Z. Naturforsch. A* **25**, 1431 (1970); M. E. ANTADZE, V. N. ROZHANSKII, G. V. TSAGAREISHVILI, AND F. N. TAVADZE, *Bor'ba Poluch. Strukt. Svoistva Mater. Mezhdunar. Simp. Boru 4th*, 54 (1974).
6. F. N. TAVADZE, G. V. TSAGAREISHVILI, N. A. ZOIDZE, AND M. E. ANTADZE, *Electron Technol.* **3**, 127 (1970).
7. E. AMBERGER, W. DIETZE, J. JAUMANN, AND P. RUNOW, *Phys. Status Solidi A* **2**, K59 (1970).
8. E. STORMS AND B. MUELLER, *J. Phys. Chem.* **82**, 51 (1978).
9. S. IIJIMA, *Acta Crystallogr. Sect. A* **29**, 18 (1973).
10. A. RAE SMITH AND L. EYRING, *Ultramicroscopy* **8**, 65 (1982).
11. J. M. COWLEY AND A. F. MOODIE, *Acta Crystallogr.* **10**, 609 (1957).
12. J. C. H. SPENCE, *Acta Crystallogr. Sect. A* **34**, 112 (1978).